Identification of the electronic structure differences between polar isostructural FeO and CoO films by core-level soft x-ray spectroscopy

Sarp Kaya,[1,2,*] Toyli Anniyev,[3,4] Hirohito Ogasawara,[2] and Anders Nilsson[1,2,3]

[1]*SUNCAT Center for Interface Science and Catalysis, SLAC National Accelerator Laboratory, 2575 Sand Hill Road, Menlo Park, California 94025, USA*

[2]*Stanford Synchrotron Radiation Lightsource, SLAC National Accelerator Laboratory, 2575 Sand Hill Road, Menlo Park, California 94025, USA*

[3]*Stanford Institute for Materials and Energy Sciences, SLAC National Accelerator Laboratory, 2575 Sand Hill Road, Menlo Park, California 94025, USA*

[4]*Department of Physics, Stanford University, Stanford, California 94305, USA*

(Received 13 November 2012; revised manuscript received 21 March 2013; published 13 May 2013)

The electronic properties of the FeO and CoO single layer thin films on Pt(111) were examined by core-level soft x-ray spectroscopy. These oxygen terminated films are bilayer-thick and isostructural Pt, Fe-Co, and O atoms stacked with small lateral shifts due an incommensurate relation with Pt(111). Probing occupied and unoccupied states projected on the oxygen atoms revealed states at the Fermi level, suggesting orbital mixing with the metal substrate, and also indicated an anisotropy in transition metal-oxygen bonding geometry. The differences in the core-level spectral features were attributed to the substrate induced modification of the charge transfer energy and with an additional valence electron on Co.

DOI: 10.1103/PhysRevB.87.205115 PACS number(s): 73.20.At, 78.70.Dm, 78.70.En

I. INTRODUCTION

The late transition metal (TM) monoxides are of great interest owing to their importance in catalysis, mineralogy, and device electronics. Particularly, the nature of the (111) terminations is characterized with the polarity that they possess. The alternating layers of 3*d* TM and oxygen atoms accumulating polarity perpendicular to the surface play an important role in material properties but also create stability problems. The free energy requirements of the polar system force the surfaces to compensate the charge built up by structural and electronic modifications. The compensation channels include (i) the surface reconstructions involving charge redistribution, (ii) anion-cation vacancy generation leading to changes in surface stoichiometry, and (iii) adsorption of foreign species.[1] Theoretical treatments are also challenging, since correlated electron systems make simple approaches fail for estimating standard electronic properties.[2,3] Interestingly, thin films with uncompensated polarity have been found to be stable if their thickness is below a critical value;[4] there are, however, deviations from the bulk values in terms of interatomic distances and electronic band gaps.

FeO and CoO are within the 3*d* TM monoxide family, whose ground state electronic configurations for Fe^{2+} and Co^{2+} are d^6 and d^7, respectively. They have been classified as charge transfer insulators in the Zaanen-Sawatzky-Allen phase diagram,[5] since the band gaps of the late TM monoxide compounds are found to be smaller than a Mott insulator could have.[6] Recent reports show that the band gaps of the bulk FeO and CoO are 2.4 eV[7] and 2.6 eV,[8] respectively. This is also contrary to the classical band theory estimations which dictate that the 3*d* TM monoxides with unfilled 3*d* states must be metallic. Hubbard theory describes this controversy by introducing the *d*-*d* Coulomb interaction energy (U_{dd}). However, it is not fully successful to give a full electronic structure picture, especially of the late TMs. Better agreements (based on the Anderson impurity model) have been achieved by introduction of the charge transfer energy (Δ), the energy required for transferring a charge from the oxygen ligand to the metal 3*d* states and by including the hybridization strength (T) between O 2*p* ligand and TM 3*d* states. These Coulomb electron correlation and ligand charge fluctuations have generally been denoted by $d^n d^n \rightarrow d^{n-1} d^{n+1}$ and $d^n \rightarrow d^{n+1}\underline{L}$, respectively, where $\underline{L}$ is a hole in the oxygen ligand. The values of U and Δ relative to the bandwidths of the TM 3*d* (w) and O 2*p* (W) valence states determine if the electronic structure of the TM complex is a conductor, Mott, or charge transfer insulator type.[5,9]

Thin oxide films grown on metallic substrates have brought a unique concept for studies using surface science techniques utilizing primarily the analysis of low energy electrons since the charging issues can be circumvented.[10] The attractiveness of these systems owing to the resemblance of bulk materials in terms of electronic and geometric structures has been balanced with the discussion regarding the influence of the substrate to those properties.[10] The electronic structures modified by hybridizations with the substrates might deviate from the bulk, however, it has also been considered to be a design parameter of catalytic systems with superior performance.[11] In the present study our main interest is on the electronic structure of FeO and CoO thin films, which have been grown on several substrates. Early successful attempts include Mo(100),[12] Fe(110),[13] and Cu(110)[14] for FeO and Co(0001),[15] Au(111),[16] and Ir(100)[17] for CoO films. Among these, Pt(111) is the unique substrate on which both films can be grown epitaxially with minor structural differences.

The structural characterizations of FeO(111) and CoO(111) epitaxial thin films grown on Pt(111) substrates have been performed in detail. Both TM monoxide films are single TM-O bilayer thick and oxygen terminated; the metal atoms decorate the interface layer with the same periodicity. The findings of earlier photoelectron diffraction (PD),[18] low energy electron diffraction (LEED), and scanning tunneling microscopy (STM)[19] studies mostly agree with the recent ones,[20] in that the FeO films grown on Pt(111) have a

lattice mismatch which is revealed as a superstructure (moiré patterns). X-ray photoelectron spectroscopy (XPS) studies show that the oxidation state of Fe is 2+, indicating the formal charges are close to the charges in FeO stoichiometry.[21,22] CoO grows on Pt(111) similarly,[23] with the Co possessing formal charges close to those in bulk CoO,[24] but much less is known about the electronic structure of this film.

As an alternative to the electronic structure understanding based on bulk materials, these films can be also viewed as oxygen atoms chemisorbed on threefold sites of 3*d* TM monolayer films. The *d*-band model[25,26] which correlates the width and the energy position of the valence electron states with the adsorbate states could in principle be adapted to describe the electronic structure and the bonding between TM and O atoms. The latter approach deals with the covalency of the chemical bond, and thus the strength of the hybridization between TM and oxygen valence states determines the electronic structure of the films. The nature of the chemical bonding between TM and O atoms can be thus defined by bonding and antibonding states of oxygen atoms. It is not clear if the electronic structures of these films are analogous to the bulk properties which are described by a small band gap. Moreover, polarity is associated with Coulomb repulsion and band filling;[27] the anisotropy in TM-O bond distances and orbital symmetry are the factors defining overall stability of these films. Core-level (CL) x-ray spectroscopy sheds light on the electronic properties since valence band (VB) and bonding configurations could be probed selectively on various atomic sites.

In this paper, we report on the differences in the electronic structures of FeO and CoO isostructural films grown on a Pt(111) substrate. We adopt CL spectroscopy techniques [x-ray absorption spectroscopy (XAS), x-ray emission spectroscopy (XES), and XPS] in order to identify the differences in an atom specific way. We show that valence electronic structures of these films differ from the bulk and the major factor that separates CoO from FeO is the additional valence electron on Co.

II. EXPERIMENT

The experiments were performed at the elliptically polarized undulator (EPU) beamline 13-2 at Stanford Synchrotron Radiation Lightsource (SSRL). The ultrahigh vacuum (UHV) endstation with a base pressure better than 2×10^{-10} Torr is equipped with an electron energy spectrometer (Scienta R3000), a high throughput slitless x-ray emission spectrometer, LEED optics (SPECS), *e*-beam evaporator (EFM 3, Omicron), and standard tools for sample cleaning. The x-ray emission spectrometer is a homebuilt grazing incidence grating spectrometer with a multichannel-plate detector. A nickel-coated spherical-elliptical grating with a 1100 lines/mm groove density was used. The curvature of the grating was 5 m and the length was 10 cm, giving an energy resolution of 0.6 eV. Sample heating was performed by a standard electron bombardment method, by accelerating electrons emitted from a filament placed on the backside of the sample. The temperature was measured by a *K*-type thermocouple that was spot welded onto the side of the sample.

The Pt(111) single crystal was cleaned by repeated cycles of Ne^+ ion bombardment and annealing to 1150 K. Segregated carbon impurities were burned off by exposing the surface to O_2 while cooling down (from 800 to 400 K). Long range order and surface cleanness were confirmed by the hexagonal (1×1) sharp LEED patterns and XPS, respectively. FeO and CoO films were prepared by depositing Fe and Co metals using an *e*-beam evaporator at room temperature and subsequent annealing in 1×10^{-6} Torr O_2 for 1 min. Annealing was performed at 950 K in the FeO case and at 840 K for CoO. The background O_2 was pumped out as the sample temperature went below 400 K. During metal deposition the sample was positively biased in order to prevent sputtering by a small amount of ionized metal atoms. The deposition rate was controlled by monitoring the ion flux. Due to the two-dimensional growth nature of the films, the film completeness could be confirmed by titrating uncovered regions of the Pt(111) surface by adsorbed CO. No CO adsorption was observed on both oxide surfaces at room temperature. Gases were dosed into the system by variable leak valves.

The electron binding energies reported here are referenced to the Fermi level of Pt(111). O *K*-edge XAS spectra were obtained by the Auger electron yield method (AEY). Spectra were recorded by placing the kinetic energy window of the spectrometer on the O *KVV* Auger transition line. Fe and Co *L*-edge XAS measurements were performed similarly, using the energy window of the *LMM* Auger transition. In-plane and out-of-plane valence orbital components for O $1s \rightarrow 2p$ and Fe-Co $2p \rightarrow 3d$ excitations were probed by rotating the sample with respect to the polarization **E** vector of the synchrotron radiation light. All XAS spectra were normalized to the incident photon flux and the background from pure Pt(111) was subtracted. O *K*-edge XES spectra were recorded by adjusting the grazing incidence angle on the grating to 5°. The excitation energy was set to the first absorption resonance as determined by XAS. In the O *K*-edge XE process the **E** vector of the emitted light is aligned with the O $2p$-projected valence orbital. Emission from O $2p_x + 2p_y$ and $2p_x + 2p_y + 2p_z$ orbitals was achieved by recording in XES in normal and grazing emission geometry, respectively.[28] In all XPS, XAS, and XES measurements the grazing incidence angle of the incoming synchrotron light was 4°.

III. RESULTS

LEED patterns obtained from FeO and CoO bilayers are shown in Fig. 1(a). The analysis of the hexagonal diffraction spots gives rise to Fe-O and Co-O in-plane lattice parameters of 3.08 and 3.13 Å, respectively, similar to the ones obtained in previous studies.[18,23] As better visualized on the model drawing of these systems in Fig. 1(a), the moiré superstructure is also well reproduced; a 11% and 13% planar and 0.6° rotational lattice mismatch with Pt(111) gives rise to the moiré periodicity of 26.3 Å in the FeO case, which is slightly shorter in the CoO case (23.9 Å).

TM $2p$ XPS spectra from FeO and CoO shown in Fig. 1(b) are characterized by spin-orbit splitting into $2p_{1/2}$ and $2p_{3/2}$ components, the energy difference between which increases from 13.4 to 15.7 eV with increasing atomic number. The interference of the satellite components with the main lines complicates the spectral analysis of many 3*d* transition metal oxides,[9] however, the sharpness of the Co $2p_{3/2}$ main line component is pronounced. The main component of Fe $2p_{3/2}$

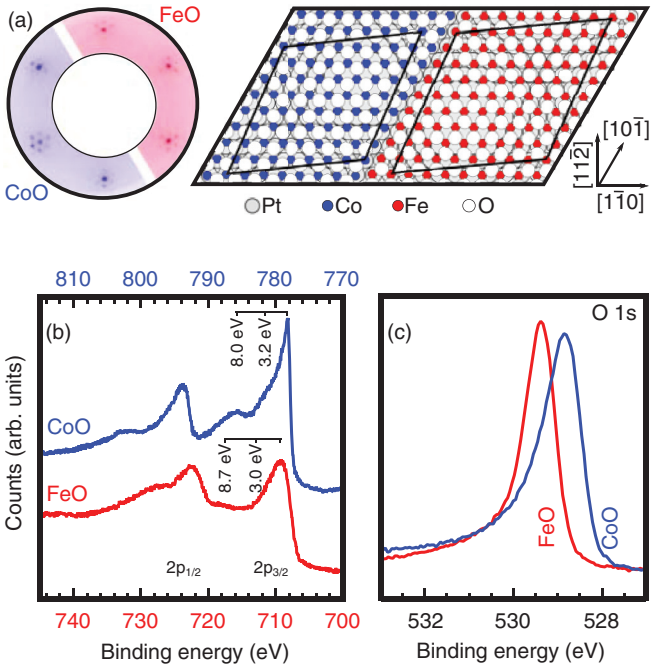

FIG. 1. (Color online) (a) LEED pattern and structural model of FeO and CoO films grown on Pt(111). Patterns were obtained by setting the kinetic energy of the incident electrons to 95 eV. (b) Co and Fe $2p$ XPS spectra recorded using photon energies of $h\nu = 880$ and 940 eV, respectively. (c) O $1s$ XPS spectra of the respective films. They are both recorded using the same photon energy, $h\nu = 700$ eV. Red and blue represent the pattern, atom, and spectrum of FeO and CoO, respectively.

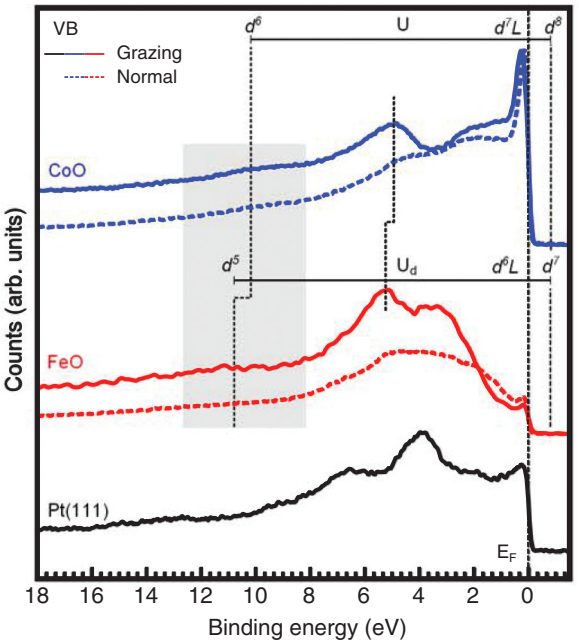

FIG. 2. (Color online) Valence band XPS spectra of FeO (red), CoO (blue), and pure Pt(111) (black) recorded at a photon energy $h\nu = 165$ eV. Normal emission spectra (dotted) labeled separately from grazing emission spectra (solid) which was measured by setting the electron take-off angle to 79° from the surface normal. Final states are denoted on the respective spectra.

located at 709.2 eV is followed by two higher binding energy (BE) components, separated from the main line by 3.0 and 8.7 eV, respectively. Similarly, the sharp main line of the Co $2p_{3/2}$ spectrum at 778.2 eV is broadened by a high BE shoulder centered at 3.2 eV and a higher BE third component is also seen at 8.0 eV. The BE of the O $1s$ line of FeO is found to be higher than that of CoO, as shown in Fig. 1(c). The O $1s$ XPS spectrum of FeO has a main component at 529.4 eV with an asymmetric tail at the low BE side. The full width half maximum (FWHM) is 0.9 eV. More asymmetry is observed in CoO; here FWHM is found to be 1.15 eV with the main line centered at 528.9 eV.

VB XPS spectra of FeO and CoO including a pure Pt(111) surface are shown in Fig. 2. The measurements were performed by setting the excitation energy close to the Cooper minimum ($\sim h\nu = 200$ eV) of the Pt $5d$ states[29] so that their contribution to the overall VB spectra is minimized. The combination of normal and grazing detection geometry along with low kinetic energy additionally provides identification of oxide related spectral features, which overlap with the Pt $5d$ states of the underlying Pt substrate. In normal geometry, distinct spectral features from O $2p$ and Fe-Co $3d$ are observed, however, in grazing geometry the substrate contribution is nearly vanished. Both FeO and CoO VB contain three distinguishable spectral features, one of which is in close proximity to the Fermi edge. The intensity of this peak is rather pronounced in CoO. The second clearly identifiable peak resides at 5.3 eV in FeO and 4.9 eV in CoO. The region between these two can be realized by a third component. In the case of FeO, the peak at 3.4 eV seems to be sharper as compared to CoO. Nevertheless, a peak centered at 2.1 eV is seen in CoO. The intensity analysis[30] performed by including the ionization cross sections,[29] electron inelastic mean free paths,[31] and electron emission geometry reveals that, in grazing geometry, the TM $3d$ contribution dominates the VB spectra. For FeO and CoO films the TM $3d$/Pt $5d$ intensity ratios are estimated to be 16.2 and 21.6, respectively. The contribution of the O $2p$ states is less pronounced, but should be detectable.

VB spectra shown in Fig. 2 involve information regarding the electronic properties of these films, however, overlapping TM $3d$ and O $2p$ states make the spectral characterization nontrivial. The atom specific approach to probe the electronic structure of these films is to take advantage of the dipole transitions, $1s \rightarrow 2p$ and $2p \rightarrow 1s$ in the case of O K-edge absorption and emission measurements, respectively. Occupied and unoccupied p states projected on the oxygen atoms of these films can then be identified. The $2p_x + 2p_y$ and $2p_z$ symmetry resolved XES and XAS spectra from FeO and CoO films are shown in Fig. 3. Spectra were aligned with respect to each other in the BE scale so that a direct comparison can be made.[32] The Fermi edge is determined by using the peak maxima of the O $1s$ XPS spectra from respective films.[28] Certain differences in spectral weights are apparent. XAS shows states above the Fermi level, a clear signature of the covalent interaction of the TM-O bonding complex. Another important finding to note here, unlike bulk oxide electronic structures, is that the FeO and CoO films on Pt(111) surfaces have states tailing near the Fermi level. The main bonding components of O $2p_x + 2p_y$ and O $2p_z$ states are at 5.6–4.1 and 5.1–4.0 eV below the Fermi level for FeO and CoO films,

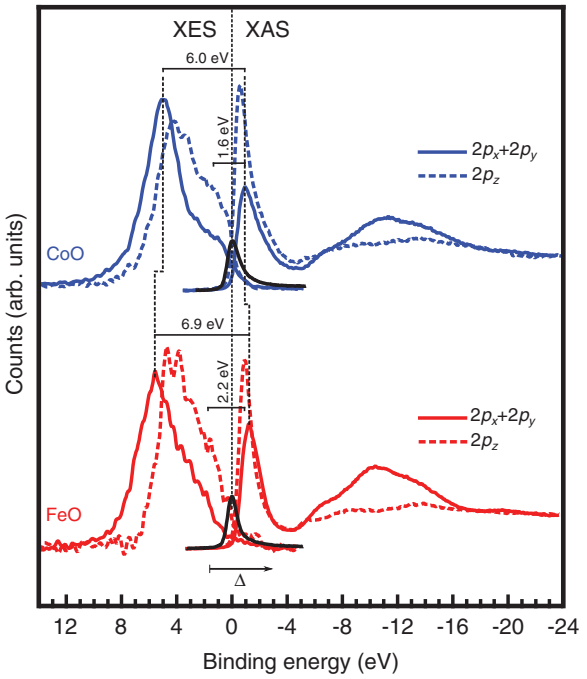

FIG. 3. (Color online) O K-edge absorption and emission spectra obtained from FeO and CoO films. The spectra were aligned in the BE scale using O 1s XPS presented in Fig. 1(c). Spectra representing $2p_x + 2p_y$ (normal), $2p_z$ (grazing) symmetry components are shown as solid and dotted lines, respectively.

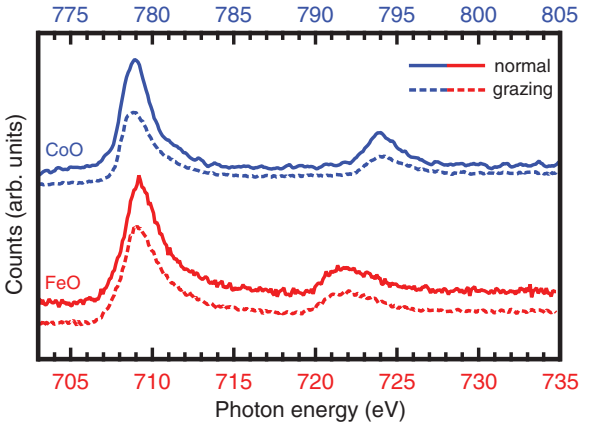

FIG. 4. (Color online) Fe and Co L-edge XAS spectra obtained from FeO and CoO films. They were recorded in two geometries and shown spectra represent unoccupied 3d states hybridized with O $2p_x + 2p_y$ (normal) and O $2p_z$ (grazing) states.

respectively. All spectra have a low BE shoulder spanning up to the Fermi level. Spectral weights of the shoulders of the O $2p_z$ states are more pronounced, and CoO seems to have more states near the Fermi level compared to FeO. The first sharp state with an antibonding character above the Fermi level is attributed to O 2p-TM 3d hybridized states. FeO has intrinsically sharper peaks and the energy difference between the resonant maxima of $2p_x + 2p_y$ and $2p_z$ is 0.4 eV. This difference becomes 0.3 eV in CoO, $2p_z$ of which is also closer to the Fermi level. The energy window covering 4–16 eV above the Fermi level is dominated by O 2p-TM 4sp hybridized states; a clear distinction is that the $2p_x + 2p_y$ components are more intense as compared to $2p_z$. The main peak of FeO is at 10.5 eV, and that of CoO is at a slightly lower energy. Nevertheless; the broad widths of these peaks make a direct comparison difficult.

TM L-edge XAS spectra of these films are relatively less complex due to a single cation valence structure. Figure 4 shows the Fe-Co L-edge XAS spectra for respective oxide films with an in-plane and out-of-plane **E** vector to the projected TM 3d component. On the L_3 edge, the CoO spectra width is relatively narrower compared to FeO, which has a prominent shoulder tailing the low energy side. This pre-edge component is almost absent in CoO. In both films, the L_3 edge can also be interpreted as a main peak with a shoulder on the high photon energy side. On the L_2 edge, the peaks are broad and featureless, however, a spectral width comparison reveals a sharper Co L_2 edge. No strong polarization dependence is observed.

IV. DISCUSSION

One of mutual structural properties of these films is oxygen termination. Previous studies indicate that the main characteristic is the out-of-plane TM-O interatomic distance that is approximately 50% shorter relative to the bulk values. There are also other differences: The electronic structures of these FeO and CoO films grown on Pt(111) surfaces can be separated from each other by the valence electronic properties of the TMs, with Co having an additional valence electron than Fe. The moiré periodicity of FeO is slightly longer but the differences in the in-plane metal-oxygen bond lengths are too small, and thus have little impact on the overall electronic structure. The registry with the Pt(111) substrate, however, slightly modifies the out-of-plane TM-O bond length. Interfacial metal atoms can be found on threefold fcc, hcp, and top sites of the Pt(111) surface and their effects are translated into the moiré superstructure observed on these films.[33] It has been shown by STM studies that the surface potential of the FeO films becomes modulated due to corrugation of the moiré superstructures.[20,34] Despite the lack of information that quantifies the variation of the surface potential of CoO films, a similar behavior is expected.

For bulk FeO and CoO, the charge transfer energy is moderate ($W/2 < \Delta < U_{dd}$),[9] and the O 2p valence states overlap with the TM 3d states. It is therefore important to separate out the TM and ligand states in order to make electronic structure comparisons viable. We have shown that O K-edge XES selectively probes O 2p states, and their contribution to the overall valence structure can be singled out by VB XPS. In the case of thin films a modified picture must be considered; valence states of the films will be overlapping with those of Pt.

These parameters can be approximated by the analysis of CL and VB XPS spectra. The satellite features observed in 2p XPS spectra of the late TM monoxide compounds have been attributed to a charge transfer mechanism, from the ligand to the metal site, and to the multiplet effects,[35] however, this approach has been challenged since it neglects the angular momentum coupling of the TM 3d electrons and

ionized core levels.[36] The late 3d TM monoxides have shown a complex behavior to the sudden creation of a core hole, suggesting differences in their VB structures. The final state of the photoemission process contains a core hole which is coupled with the partially filled TM 3d states, giving rise to mainline broadening and satellite features in XPS spectra depending on the particular overlap between core levels and the valence states. These multiplet effects are represented by U_{cd}, with c being the core hole states (the change in the VB electronic configuration is alternatively illustrated by a $Z+1$ approximation, where Z is the atomic number).[37,38] The extent of the spatial interaction between orbitals can be directly reflected to the XPS spectra. Resonant and nonresonant photoemission studies have also shown a 3s3p-3d overlap which leads to the satellites and resonant enhancements, however, multiplet effects can be translated as spectral broadening in TM 2p XPS spectra due to a smaller overlap between the 2p hole and 3d orbitals.[39] It must therefore be noted here that the analysis of CL 2p spectra does not directly provide U_{dd} and Δ parameters, which can be better described in ground state electronic structures. When a 2p core hole is created, two final state electronic configurations are described by cd^n and $cd^{n+1}\underline{L}$, and the energy difference between these two final states, $U_{cd}-\Delta$, determines the BE of the satellite peaks. The satellites of the TM 2p XPS spectra presented in Fig. 1(b) indicate a similar mechanism, the involvement of at least two different final states. Another point to note is the relative intensities: The satellite features of FeO seem to have a more pronounced intensity (although smeared out) compared to the main well-screened line. These differences are attributed to the screening efficiency of the metallic substrate. The efficiency of the hole screening is evidenced by the sharpness of the Co 2p XPS peaks, also suggesting metallic behavior. In addition, the BE of the Co 2$p_{3/2}$ main line peak position appears to be slightly lower than the BE of Co^{2+} of the bulk systems.[9] Despite the differences in the intensity ratios of the main lines to the satellite peaks, the $c(4\times2)$ and (9×2) phases of the cobalt oxides grown on Pd(100) demonstrate similar BEs.[40] The XPS spectrum of FeO films is identical to the previously published data.[21]

The 2p XPS spectra of FeO and CoO show two peaks separated by $U_{cd}-\Delta$, the energy difference between unscreened and well-screened cd^6 and $cd^7\underline{L}$ final states in FeO, and the difference between cd^7 and $cd^8\underline{L}$ final states in CoO. The shoulders residing on the ~3 eV high BE side of the well-screened main lines are attributed to the multiplet effects which are stronger in 2$p_{3/2}$ states than 2$p_{1/2}$.[41] By comparing the relative intensities and the energy differences between the main and satellite peaks presented in Fig. 1(b) with the previously reported spectra from bulk samples, one can notice certain differences.[39,42] The satellites of the thin films seem to be less pronounced and $U_{cd}-\Delta$ values are relatively larger. It is worthwhile to point out that structure mediated hybridization shifts are also involved in the energy separation. It has been reported that $U_{cd}-\Delta$ obtained from 2p XPS spectra of bulk FeO and CoO is 6.04 and 5.8 eV, lower than the energy differences that thin films display (8.7 and 8.0 eV). This would suggest that U and Δ are modified for the thin films due to their image dipoles on metal substrates.

Electronic and magnetic properties of the late TM oxides grown on metal substrates differ since the Coulomb and charge transfer energies in thin films have smaller values due to efficient image potential screening.[43] The reduction in Δ has been proposed to be the main contributor to the larger energy separation between the main and the satellite peaks ($U_{cd}-\Delta$), mainly in connection to the possibly lower Madelung potential. U_{cd} remains larger than the d-band width w despite an orbital overlap with the substrate, and the effect of the core hole can be assumed to be unchanged since screening takes place from the VB of the same atom. The intensities of the satellite peaks are also expected to be more pronounced under the circumstances where Δ is reduced (in the presence of the core hole).[44] The origin of the discrepancy of the ratio of the satellite to main peaks between the thin films and the bulk samples is the effect of the hybridization strength[45] between the TM 3d and O 2p states, which is enhanced due to the shorter out-of-plane TM-O bond lengths and also due to the lateral strain in the film (the influence of the latter is expected to be weaker since the bond lengths of the former are more modified). The hybridization effect is also evident from the VB XPS and XES spectra: The energies of the O 2p and TM 3d states significantly overlap in the range below the Fermi level. A larger peak difference in FeO compared to bulk could thus reflect the different Fe-O bond lengths. Moreover, the contribution of the Pt 5d-TM 3d/O 2p spatial overlap is not insignificant, as it will be discussed below in the analysis of the VB structures.

The effect of the screening manifests itself in the O 1s XPS spectra shown in Fig. 1(c). The O 1s BE of CoO is found to be 0.5 eV lower than that of FeO, which has not been the case for bulk monoxides. A lower O 1s BE has been observed in MnO, but FeO, CoO, and NiO have O 1s XPS spectra with rather similar binding energies.[42] This situation is unique for monolayer thin oxide films grown on metallic substrates, where, by increasing the layer thicknesses, the electronic properties converge to the bulk behavior, and thus XPS spectra of the films thicker than five atomic layers are expected to become identical to the bulk.[46,47] The energy of the oxygen ligand at the final state determines the O 1s BE, which is different in these two situations, and the evidence of the difference is the O 2p electronic structure presented in O K-edge XES spectra. Although the LEED pattern shows perfect long range order, CoO films could be slightly more defective at the atomic scale and it might give rise to the larger FWHM. However, the presence of the other species such as hydroxyl groups (–OH) must be ruled out since no XES-XAS spectral features that could point to their existence have been observed.

The charge transfer energy Δ can be approximated as the electron-hole pair excitation between the lowest unoccupied and the highest occupied states in the O 2p-TM 3d hybridized system. This can be obtained from O K-edge XES and XAS spectra by taking the energy difference between the lowest unoccupied and the highest occupied states. The highest lying occupied O 2p state can be directly obtained, however, one needs to assume that the O 2p-TM 3d hybridized state in the absorption spectra determines the lowest unoccupied state of the metal site. Another important caution that one needs to take into account is the final state effects in x-ray absorption

and emission processes. In the absorption event the final state has an O $1s$ core hole whereas the core hole is filled in the emission event. The presence of the core hole in the final state generally shifts XAS spectra to lower BE and excitonic effects could potentially modify the intensity of the XAS peaks.[48] Therefore, approximated Δ values are probably lower than the values reported in the literature and in the present work. Nevertheless, following this approach, the change in Δ in bulk samples has been found to be in the order along which the systems become more ionic: NiO < CoO < MnO; 5.4, 6.1, and 6.6 eV, respectively.[8] The examination of the electronic structure shown in Fig. 3 reveals that the energy separation between the oxygen bonding and the antibonding states is much smaller compared to the bulk samples; 2.2 eV (FeO) and 1.6 eV (CoO) are the approximated Δ values of bilayer films. More importantly, the density of states (DOS) near the Fermi level is nonvanishing, further suggesting a deviation from the bulk electronic structures. Larger Δ values with a decreasing atomic number of the $3d$ TM are consistent with the trend in the bulk TM monoxides.[8,39] This indicates that image dipole and hybridization causes a reduction in Δ; the trend among $3d$ TM monoxide films is persistent, provided that they are isostructural.

The distribution of O $2p$ and TM $3d$ DOS over the occupied part of the band structure can be identified by a comparison of VB XPS (Fig. 2) with O K-edge XES (Fig. 3). The XES spectral signatures arise from a hybridized TM-O chemical bond resulting in bonding and antibonding orbitals of oxygen atoms. In bulk FeO and CoO, TM cations have an octahedral symmetry, surrounded by six oxygen anions. In this configuration the TM $3d$ orbital splits into two bond configurations, σ (e_g: $d_{x^2-y^2}$, d_{z^2}) and π (t_{2g}: d_{xy}, d_{xz}, d_{yz}), where the TM-O hybridization strength differs due to bond anisotropy. The energy differences between these two levels depend on the number of d electrons in the ground state and also on the TM-O chemical bond length. The orbital overlap on (111) plane of the thin films will have a similar interpretation. The interactions on the (111) plane induce a stronger overlap between the O $2p$ and TM $3d$ orbitals. One can also view this system as a monolayer of oxygen atoms bound to the threefold sites of the monolayer TM film. In an fcc hollow site, the O $2p_x$-$2p_y$ orbitals are involved more in the chemical bonding, where the largest orbital overlap with TM $3d$ orbitals occurs through the σ interaction between TM $3d$ ($d_{x^2-y^2}$, d_{xy}) and O $2p$ orbitals, whereas perpendicular to the (111) plane the π bonding interaction between the O $2p_z$ and TM $3d$ (d_{xz}, d_{yz}, d_{z^2}) orbitals is realized.[49] A larger overlap for the σ interaction in the (111) plane translates into a larger energy separation between the bonding and antibonding states as observed in the XES and XAS spectra. The bond strength of TM-O can thus be estimated by comparing the energy difference, and the stronger Fe-O interaction gives rise to an energy separation (6.9 eV) larger than Co-O (6.0 eV). As in both cases O $2p$ states spill over the Fermi level.

The broad peaks covering the 5–8 eV energy range in VB spectra in grazing geometry shown in Fig. 2 are straightforwardly assigned to O $2p$ states, but the region below 5 eV is more difficult to interpret due to the mixed TM $3d$-O $2p$ states. VB spectra qualitatively agree with the previous studies,[21,40,50,51] and in the present work the spectral features are much better resolved. Pt $5d$ states still contribute to the spectra taken in normal electron emission geometry whereas they nearly vanish in grazing geometry. As in XES spectra, O $2p$ derived states in FeO (5.3 eV) shift to a lower BE in CoO (4.9 eV). Previous resonant photoemission studies at the TM $3p \rightarrow 3d$ absorption threshold identified the resonant enhancements of $3d$ derived states in VB XPS spectra.[50,51] In light of these studies, the sharp peak just 1 eV below the Fermi edge, broad peaks covering the 1–4 and 8–14 eV energy region are assigned to TM $3d$ states, the former with strongly hybridized characteristics. The peak at $\sim$1 eV is assigned to a well-screened $d^n\underline{L}$ ($n = 6, 7$ in FeO and CoO) level at the final state. Apparent intensity domination of this peak in CoO also puts forward the effect of the hybridization with the oxygen states, an observation in line with XES spectra. The rather broad peaks, $\sim$10.8 eV (FeO) and 10.2 eV (CoO), below the Fermi edge are attributed to d^{n-1} final states. Despite their weak intensity observed here, their existence as a photoionized final state has been justified by the resonant and angle resolved photoemission studies.[50–52] The energy difference between these high BE peaks and the first TM $3d$ absorption resonance peak above the Fermi level (presumably at the same energy as the first resonance in O XAS) corresponds to U_{dd} and it is certainly higher than 11 eV. This value is in the range of Coulomb energies estimated and calculated for late TM monoxides[51] and also quite larger than charge transfer energies. This result indicates that our initial assumption of U being unchanged due to image charge screening is reasonable.

O K-edge and TM L-edge XAS spectra presented in Figs. 3 and 4 highlight the anisotropy of the hybridization between orbitals. The first resonant feature is larger in width compared to the pure metal L-edge spectra,[53] but π^* and σ^* antibonding states are not seen clearly. This indicates that the crystal field is not as strong as in the case of bulk TM monoxides. The FWHM of the first resonance peaks in FeO seems to be larger, suggesting that the energy difference between σ^* and π^* orbitals is larger. This is indeed confirmed by O K-edge XAS: The first resonance in $2p_x + 2p_y$ symmetry resides at a 0.3 eV higher energy than the one in $2p_z$. The $2p$-$4sp$ hybridized peak at $\sim$10 eV above the Fermi edge is more intense in FeO and thereby the bonding interaction on (111) plane is stronger.

Symmetry resolved intensity differences in XAS spectra also reveal that the TM-O bond geometry is more anisotropic in CoO. This comparison is basically based on the similar bulk lattice parameters, and on an ideal monoxide structure where TM is octahedrally coordinated to the oxygen anions. It can be attributed to the lateral strain, as a consequence that the Co-O lattice is extended more out of plane. The anisotropy in the bond symmetry can also be attributed to more pronounced O $2p$ states right below the Fermi level, as shown by XES. Nevertheless, both films show a structural resemblance but their electronic properties are slightly different with respect to each other.

V. CONCLUSIONS

Core-level spectroscopy has been utilized to characterize the electronic properties of polar FeO and CoO single TM-O bilayer-thick, isostructural films grown on Pt(111). The

differences in the core-level spectral features of these films scale well with the spectra obtained from bulk samples, but deviations between the TM monoxides of the same metals are related to the screening and bonding properties of substrate metal. In addition, TM-O interatomic distances contribute to the modified electronic structures of the FeO and CoO films and consequently their influence is reflected in the core-level spectral features. The oxygen density of states below and above the Fermi level and overall valence band electronic structure give evidence that the electronic states of these films are strongly coupled with the Pt substrate states. The conclusions drawn here may potentially play an important role in understanding the magnetic, electronic, and surface chemical properties of TM monoxides on metallic substrates. These oxides are also active towards certain surface chemical reactions, such as the oxygen evolution reaction of importance in water splitting and the Fischer-Tropsch process for the synthesis of hydrocarbons; modified bond lengths imply that these thins films are involved in oxidation reduction surface chemical cycles in different ways.

ACKNOWLEDGMENTS

This work was supported by the US National Science Foundation, through Grants No. CHE-043142 and No. CHE-0809324. Portions of this research were carried out at the Stanford Synchrotron Radiation Lightsource, a Directorate of SLAC National Accelerator Laboratory and an Office of Science User Facility operated for the US Department of Energy Office of Science by Stanford University.

*Corresponding author: sarpkaya@slac.stanford.edu

[1] D. Cappus, M. Hassel, E. Neuhaus, M. Heber, F. Rohr, and H. J. Freund, Surf. Sci. **337**, 268 (1995).
[2] P. W. Tasker, J. Phys. C **12**, 4977 (1979).
[3] J. Goniakowski, F. Finocchi, and C. Noguera, Rep. Prog. Phys. **71**, 016501 (2008).
[4] J. Goniakowski, C. Noguera, and L. Giordano, Phys. Rev. Lett. **98**, 205701 (2007).
[5] J. Zaanen, G. A. Sawatzky, and J. W. Allen, Phys. Rev. Lett. **55**, 418 (1985).
[6] K. Terakura, T. Oguchi, A. R. Williams, and J. Kübler, Phys. Rev. B **30**, 4734 (1984).
[7] K. C. Prince, M. Matteucci, K. Kuepper, S. G. Chiuzbaian, S. Bartkowski, and M. Neumann, Phys. Rev. B **71**, 085102 (2005).
[8] E. Z. Kurmaev, R. G. Wilks, A. Moewes, L. D. Finkelstein, S. N. Shamin, and J. Kuneš, Phys. Rev. B **77**, 165127 (2008).
[9] G. Lee and S.-J. Oh, Phys. Rev. B **43**, 14674 (1991).
[10] H.-J. Freund and D. W. Goodman, in *Handbook of Heterogeneous Catalysis* (Wiley-VCH, Weinheim, 2008).
[11] Q. Fu, W.-X. Li, Y. Yao, H. Liu, H.-Y. Su, D. Ma, X.-K. Gu, L. Chen, Z. Wang, H. Zhang, B. Wang, and X. Bao, Science **328**, 1141 (2010).
[12] J. S. Corneille, J.-W. He, and D. W. Goodman, Surf. Sci. **338**, 211 (1995).
[13] K. Mori, M. Yamazaki, T. Hiraki, H. Matsuyama, and K. Koike, Phys. Rev. B **72**, 014418 (2005).
[14] E. Yagasaki and K. Kishi, J. Electron. Spectrosc. **69**, 133 (1994).
[15] M. Hassel and H.-J. Freund, Surf. Sci. **325**, 163 (1995).
[16] S. Sindhu, M. Heiler, K.-M. Schindler, and H. Neddermeyer, Surf. Sci. **541**, 197 (2003).
[17] C. Giovanardi, L. Hammer, and K. Heinz, Phys. Rev. B **74**, 125429 (2006).
[18] Y. J. Kim, C. Westphal, R. X. Ynzunza, H. C. Galloway, M. Salmeron, M. A. Van Hove, and C. S. Fadley, Phys. Rev. B **55**, 13448 (1997).
[19] M. Ritter, W. Ranke, and W. Weiss, Phys. Rev. B **57**, 7240 (1998).
[20] L. Giordano, G. Pacchioni, J. Goniakowski, N. Nilius, E. D. L. Rienks, and H. J. Freund, Phys. Rev. B **76**, 075416 (2007).
[21] T. Schedel-Niedrig, W. Weiss, and R. Schlogl, Phys. Rev. B **52**, 17449 (1995).
[22] Y. Yao, Q. Fu, Z. Wang, D. Tan, and X. Bao, J. Phys. Chem. C **114**, 17069 (2010).
[23] M. De Santis, A. Buchsbaum, P. Varga, and M. Schmid, Phys. Rev. B **84**, 125430 (2011).
[24] S. Entani, M. Kiguchi, and K. Saiki, Surf. Sci. **566-568**, 165 (2004).
[25] B. Hammer and J. K. Norskov, in *Impact of Surface Science on Catalysis* (Academic, New York, 2000), pp. 71–129.
[26] A. Nilsson, L. G. M. Pettersson, B. Hammer, T. Bligaard, C. H. Christensen, and J. K. Nørskov, Catal. Lett. **100**, 111 (2005).
[27] C. Noguera, J. Phys.: Condens. Matter **12**, R367 (2000).
[28] A. Nilsson and L. G. M. Pettersson, Surf. Sci. Rep. **55**, 49 (2004).
[29] J. J. Yeh and I. Lindau, At. Data Nucl. Data Tables **32**, 1 (1985).
[30] The contributions of Pt $5d$, TM $3d$, and O $2p$ states to the VB XPS spectra could be estimated by spectral intensity calculations taking into account ionization cross sections (σ), the inelastic mean free path of the electrons (λ), and electron emission detection geometry (θ). The intensity ratio of the spectral contribution of the films to the spectral contribution from the Pt(111) substrates is given by $I_{\text{film}}/I_{\text{Pt(111)}} = (\sigma_{\text{film}}/\sigma_{\text{Pt(111)}})\exp(d/\lambda \sin\theta)$, where d is the thickness of the FeO and CoO films. Theoretically estimated ionization cross sections at $h\nu = 165$ eV (Ref. 29) favor contributions from the films over the substrate; 14.2, 18.8, and 2.4 correspond to $\sigma_{\text{film}}/\sigma_{\text{Pt(111)}}$ obtained from (TM $3d$/Pt $5d$) and (O $2p$/Pt $5d$) of FeO and CoO films, respectively. As a first approximation the thickness of the films can be assumed to be similar and d therefore can be taken as 0.80 Å (Ref. 33). Including λ though, FeO and CoO, 6.09 and 5.75 Å (Ref. 31), respectively, 12.3:16.1:1 is obtained for a $3d/5d$ intensity fraction of FeO:CoO:Pt in normal emission geometry and the enhancement in grazing geometry is found to be 16.2:21.6:1. The contribution of O $2p$ spectra is smaller, and the $2p/5d$ intensity fractions of FeO:CoO:Pt in normal and grazing geometries are 2.07:2.05:1 and 2.74:2.76:1, respectively. The contribution of Pt $6s$ states to the VB spectra was disregarded since the ionization cross section at 165 eV is smaller than an order of magnitude (Ref. 29).
[31] S. Tanuma, C. J. Powell, and D. R. Penn, Surf. Interface Anal. **20**, 77 (1993).
[32] A. Nilsson, J. Electron Spectrosc. **126**, 3 (2002).

[33]W. H. Zhang, Z. Y. Li, Y. Luo, and J. L. Yang, J. Phys. Chem. C **113**, 8302 (2009).
[34]E. D. L. Rienks, N. Nilius, H. P. Rust, and H. J. Freund, Phys. Rev. B **71**, 241404 (2005).
[35]G. van der Laan, C. Westra, C. Haas, and G. A. Sawatzky, Phys. Rev. B **23**, 4369 (1981).
[36]P. S. Bagus, R. Broer, W. A. de Jong, W. C. Nieuwpoort, F. Parmigiani, and L. Sangaletti, Phys. Rev. Lett. **84**, 2259 (2000).
[37]S. Hüfner, *Photoelectron Spectroscopy* (Springer, Berlin, 2003).
[38]F. de Groot and A. Kotani, *Core Level Spectroscopy of Solids* (CRC, Boca Raton, FL, 2008).
[39]R. Zimmermann, P. Steiner, R. Claessen, F. Reinert, S. Hufner, P. Blaha, and P. Dufek, J. Phys.: Condens. Matter **11**, 1657 (1999).
[40]L. Gragnaniello, S. Agnoli, G. Parteder, A. Barolo, F. Bondino, F. Allegretti, S. Surnev, G. Granozzi, and F. P. Netzer, Surf. Sci. **604**, 2002 (2010).
[41]K. Okada and A. Kotani, J. Phys. Soc. Jpn. **61**, 4619 (1992).
[42]F. Parmigiani and L. Sangaletti, J. Electron Spectrosc. **98-99**, 287 (1999).
[43]S. Altieri, L. Tjeng, and G. Sawatzky, Thin Solid Films **400**, 9 (2001).
[44]J. Zaanen, C. Westra, and G. A. Sawatzky, Phys. Rev. B **33**, 8060 (1986).
[45]A. E. Bocquet and A. Fujimori, J. Electron. Spectrosc. **82**, 87 (1996).
[46]S. Altieri, L. H. Tjeng, F. C. Voogt, T. Hibma, and G. A. Sawatzky, Phys. Rev. B **59**, R2517 (1999).
[47]S. A. Chambers and T. Droubay, Phys. Rev. B **64**, 075410 (2001).
[48]P. A. Brühwiler, A. J. Maxwell, C. Puglia, A. Nilsson, S. Andersson, and N. Mårtensson, Phys. Rev. Lett. **74**, 614 (1995).
[49]T. Wiell, J. E. Klepeis, P. Bennich, O. Björneholm, N. Wassdahl, and A. Nilsson, Phys. Rev. B **58**, 1655 (1998).
[50]R. J. Lad and V. E. Henrich, Phys. Rev. B **39**, 13478 (1989).
[51]Z.-X. Shen, J. W. Allen, P. A. P. Lindberg, D. S. Dessau, B. O. Wells, A. Borg, W. Ellis, J. S. Kang, S.-J. Oh, I. Lindau, and W. E. Spicer, Phys. Rev. B **42**, 1817 (1990).
[52]S. Masuda, Y. Harada, H. Kato, K. Yagi, T. Komeda, T. Miyano, M. Onchi, and Y. Sakisaka, Phys. Rev. B **37**, 8088 (1988).
[53]H.-J. Kim, J.-H. Park, and E. Vescovo, Phys. Rev. B **61**, 15284 (2000).